




Gastric Cancer Mesenchymal Stem Cells Trigger Endothelial Cell Functional Changes to Promote Cancer Progression

Linjing Cui¹ · Ting Liu¹ · Chao Huang¹ · Fumeng Yang¹ · Liqi Luo¹ · Li Sun³ · Yuanyuan Zhao¹ · Deqiang Wang² · Mei Wang¹ · Yong Ji⁴ · Wei Zhu¹ 

Accepted: 3 April 2024 / Published online: 10 April 2024

© The Author(s), under exclusive licence to Springer Science+Business Media, LLC, part of Springer Nature 2024

Abstract

Our previous studies have highlighted the pivotal role of gastric cancer mesenchymal stem cells (GCMSCs) in tumor initiation, progression, and metastasis. In parallel, it is well-documented that endothelial cells (ECs) undergo functional alterations in response to challenging tumor microenvironment. This study aims to elucidate whether functional changes in ECs might be induced by GCMSCs and thus influence cancer progression. Cell proliferation was assessed through CCK-8 and colony formation assays, while cell migration and invasion capabilities were evaluated by wound-healing and Transwell assays. Immunohistochemistry was employed to examine protein distribution and expression levels. Additionally, quantitative analysis of protein and mRNA expression was carried out through Western blotting and qRT-PCR respectively, with gene knockdown achieved using siRNA. Our findings revealed that GCMSCs effectively stimulate cell proliferation, migration, and angiogenesis of human umbilical vein endothelial cells (HUVECs), both in vitro and in vivo. GCMSCs promote the migration and invasion of gastric cancer cells by inducing the expression of Slit2 in HUVECs. Notably, the inhibition of phosphorylated AKT partially mitigates the aforementioned effects. In conclusion, GCMSCs may exert regulatory control over Slit2 expression in ECs via the AKT signaling pathway, thereby inducing functional changes in ECs that promote tumor progression.

Keywords Gastric cancer · Mesenchymal stem cells · Endothelial cells · Slit2 · AKT · Cancer progression

Introduction

Gastric cancer (GC) is a prevalent malignant tumor worldwide, characterized by high morbidity and mortality rates [1]. It is widely recognized that tumor recurrence and metastasis are not solely driven by the intrinsic behavior of tumor cells but also heavily influenced by the tumor microenvironment

(TME) [2, 3]. In addition to immune cells, TME encompasses stromal cells, fibroblasts, and endothelial cells [4]. Among the stromal cells in TME, mesenchymal stem cells (MSCs) have garnered significant attention in recent years. Accumulating evidence suggests that GC-derived MSCs (GCMSCs) possess immunomodulatory capabilities, which play a pivotal role in tumor development [5–7]. Our previous researches have demonstrated that GCMSCs exert immunosuppressive effects through the secretion of soluble factors and exosomes [8, 9], contributing to tumor immune evasion [10]. Therefore, GCMSCs significantly promote growth, metastasis and drug resistance of gastric cancer, which is a major reason for the poor prognosis of patients [9]. However, the precise mechanisms underlying how GCMSCs facilitate tumor progression remain unclear.

Cancer progression is a lethal process involving tumor cells breaking away from the primary sites, entering the bloodstream, and spreading to distant tissues and organs [11]. The pathways through which solid tumors metastasize are varied, with lymphatic spread being a primary route

✉ Wei Zhu
zhuwei@ujs.edu.cn

¹ School of Medicine, Jiangsu University, 301 Xuefu Road, Zhenjiang, Jiangsu Province 212013, China

² Department of Oncology, Affiliated Hospital of Jiangsu University, Zhenjiang, Jiangsu Province, China

³ Department of Clinical Laboratory, Affiliated Kunshan Hospital of Jiangsu University, Suzhou, Jiangsu Province, China

⁴ Department of Surgery, Jingjiang People's Hospital, Jingjiang, Jiangsu Province, China

[12], while hematogenous spread represents another significant mode of dissemination [13]. Endothelial cells (ECs) form tightly connected monolayers that line the inner surface of blood vessels [14]. They are pivotal components of the tumor microenvironment and metastatic niche [15]. Collagenase [16] and tumor growth factors produced by cancer cells [17] can directly or indirectly cause ECs activation and promote angiogenesis at the tumor site to create a favorable environment for tumor metastasis. Furthermore, proteolytic enzymes released by cancer cells can degrade the basement membrane, which consists of extracellular matrix and vascular endothelial cells [18]. This degradation enhances the penetration of tumor cells, allowing them to eventually settle in distant tissues.

It has been documented that ECs can undergo prometastatic phenotypic changes when exposed to the tumor microenvironment [19]. This transformation involves the acquisition of mesenchymal characteristics, marked by a notable increase in mesenchymal markers such as α -smooth muscle actin (α -SMA), N-cadherin (N-cad), and vimentin, along with the loss of endothelial markers like E-cadherin (E-cad) and CD31 [20, 21]. These changes are associated with enhanced endothelial cell proliferation, migration, and aggressiveness [22]. The cells take on a spindle-like shape, resulting in disorganized intercellular connections that facilitate the dissemination of tumor cells [23, 24]. Furthermore, endothelial cells within the tumor microenvironment tend to form more blood vessels, thereby providing a nutrient-rich environment that supports tumor growth [25]. Concurrently, the Slit2/Robo4 signaling pathway plays a significant role in angiogenesis and the maintenance of vascular homeostasis [26, 27]. Endothelium-derived Slit2 may serve as a recruitment signal, promoting tumor cell migration and infiltration into the vasculature [28].

The objective of this study was to examine the impact of GCMSCs on endothelial cells function and their potential role in promoting GC cell migration. The results revealed phenotypic changes in endothelial cells and an increase in the expression of Slit2, which contributed to the recruitment of more GC cells. Additionally, it was observed that inhibiting the expression of phosphorylated AKT could partially reverse this phenomenon. These findings provide new and valuable insights into a potential mechanism underlying the progression of gastric cancer.

Materials and Methods

GCMSCs, BMMSCs, Cell Lines, and Cell-Culture

GC tissues were obtained from patients undergoing surgical procedures at the Affiliated Hospital of Jiangsu University.

GCMSCs were isolated and cultured following previously established protocols [7]. Fresh tissues, cut into approximately 1 mm³ pieces, were adhered to 35 mm cell culture dishes (Corning, USA) and cultured in α -MEM (Biosharp) containing 10% fetal bovine serum (FBS, Gibco) at 37 °C in a 5% CO₂ environment. The culture medium was renewed every 3 days until fibroblast-like cells reached a confluence rate of approximately 80%. Identification of fibroblast-like cells was performed through lipogenesis and osteogenesis experiments. Flow cytometric analysis of the surface markers (CD19, CD29, CD34, CD45, CD90, and CD105) on GCMSCs was conducted [29, 30].

Bone marrow MSCs (BMMSCs) were isolated from healthy donors using the density gradient centrifugation method [31]. These cells were expanded to five passages for use in subsequent experiments. Para cancer tissues located more than 5 cm away from the tumor site were collected from the same patient as a control. Ethical approval for these procedures was obtained from the Ethics Committee of Jiangsu University, and informed consent was obtained from all subjects.

The human GC cell lines (SGC-7901, HGC-27) were cultured in RPMI 1640 medium (Gibco) with 10% FBS at 37 °C in a humidified atmosphere with 5% CO₂.

Human umbilical vein endothelial cells (HUVECs), commonly used as in vitro models of human vascular endothelial cells, were generously provided by Yan Yongmin's laboratory. These cells were cultured in high glucose DMEM medium (VivaCell) with 10% FBS for use in subsequent experiments.

Preparation of BMMSC Conditioned Medium (BMMSC-CM) and GCMSC Conditioned Medium (GCMSC-CM) and Co-Culture with HUVECs

BMMSCs and GCMSCs were cultured in cell culture flasks, and the culture medium was replenished when the cell density reached approximately 80%. After 48 h of replacing the nutrient solution, conditioned medium was collected and centrifuged at 2000 g for 10 min to eliminate cellular debris. The resulting supernatant was filtered through a 0.22 μ m membrane (Millipore, Germany) and stored at -80 °C. The supernatant was mixed with DMEM medium containing 10% FBS at a 1:1 volume ratio to create GCMSC-CM or BMMSC-CM.

When the degree of cell fusion of HUVECs reached about 70%, HUVECs were rinsed with PBS and then exposed to DMEM, GCMSC-CM, MK-2206 (10 mM, Beyotime), or GCMSC-CM combined with MK-2206 (50 nM) for 24 h in preparation for subsequent experiments.

MK-2206 is diluted with DMEM containing 10% FBS and stored at -80 °C according to the instructions.

Cell Proliferation Assay

To assess the potential impact of GCMSCs on HUVECs' proliferation, the cell counting kit-8 assay (CCK-8; Dojindo, Kyushu Island, Japan) was employed following the manufacturer's instructions. HUVECs (2×10^3 cells/well, with four replicates per group) were seeded into a 96-well plate and cultured for 24 h until they adhered to the plate. Subsequently, 10 μ L of CCK-8 solution and 90 μ L of fresh culture medium were added to each well. The absorbance at 450 nm was measured at intervals of 0 h, 24 h, 48 h, and 72 h after treatment with or without GCMSC-CM.

Wound-Healing Assay and Transwell Migration Assay of HUVECs

To evaluate the influence of GCMSC-CM on HUVEC migration, wound healing assays and Transwell migration assays were conducted. When HUVECs in a six-well plate reached 90% confluence, a sterile pipette tip was used to create an artificial wound by scratching the monolayer. HUVECs were subsequently treated with GCMSC-CM, an equal volume of serum-free DMEM, or with or without the AKT inhibitor MK-2206 (50 nM). The width of the scratch was measured 24 h later. Image J was employed to measure and calculate the area that the cells had migrated into.

For the Transwell migration assay, $0.8 \sim 1 \times 10^4$ HUVECs that had been treated differently for 24 h were suspended in 200 μ L of serum-free DMEM and placed in the upper Transwell chamber (Corning, NY, USA), which had an 8 μ m pore size polycarbonate membrane, in 24-well plates. The lower chambers were supplemented with 600 μ L of DMEM containing 10% FBS. Non-migrated cells on the upper surface of the membrane were removed softly, and cells that had migrated through the membrane were fixed with 4% paraformaldehyde and stained with 0.5% crystal violet. The number of migrated HUVECs was counted from four randomly selected fields.

Western Blotting

HUVECs were lysed on ice using RIPA buffer (Invitrogen, Carlsbad, CA, USA) containing protease inhibitors according to standard protocols. The lysates were then centrifuged at 12,000 g for 15 min at 4 °C. The protein concentration in the cell lysates was determined using the BCA Protein Assay Kit (Beyotime). A total of 20 μ g of protein samples were separated on 10% SDS-PAGE gels and subsequently transferred onto polyvinylidene fluoride (PVDF) membranes (Millipore, Billerica, MA, USA). Following blocking with 5% skim milk for 1 h, the PVDF membranes containing the target fragments were incubated with primary antibodies

overnight at 4 °C. The primary antibodies used were against E-cadherin, N-cadherin, α -SMA, ZO-1, AKT, P-AKT (all diluted to 1:1,000, Cell Signaling Technology, USA), Slit2 (1:1,000, Proteintech, USA), Vimentin (1:5,000, Proteintech, USA), GAPDH, and β -actin (1:4,000, Cell Signaling Technology, USA). Subsequently, the PVDF membranes were washed three times with TBST for 5 min each time. Goat anti-mouse and anti-rabbit secondary antibodies (both diluted to 1:3,000, Cell Signaling Technology, USA) conjugated with horseradish peroxidase were added and incubated at room temperature for 1 h. Signals were detected using ECL reagents (Millipore, Billerica, MA, USA).

Tube Formation Assay

The effect of GCMSCs on the angiogenic ability of HUVECs was evaluated by tube formation assay. A 96-well plate was added with 50 μ L/well Matrigel Basement Matrix (BD Pharmingen, San Diego, CA, USA), coagulating at 37°C for 1 h until dried. Then, HUVECs suspension (50 μ L/well) with a cell density of 2×10^4 cells were seeded on Endothelial Cell Medium (ECM) gel treated with or without GCMSC-CM in advance (four replication per group). After 4 h of incubation at 37°C, tube formations were visualized and photographed with an inverted microscope. Number of branches and total branches length of per field were calculated using Image J.

Animal Tumor Model and Tumor Tissue Immunofluorescence

4~5-week-old male BALB/c nude mice ($n=6$ for each group) were purchased from the GemPharmatech LLC (Nanjing, China). All studies performed were approved by the University Committee on Use and Care of Animals of Jiangsu University. The subcutaneous tumor models were established by injecting SGC-7901 (1×10^6). Starting from day 7, GCMSC-CM (200 μ L) was injected peritumorally every two days. An equal volume of PBS was given as a control. The mice were euthanized on day 21 after tumor transplantation, and the tumor tissue was removed for pathological section preparation. CD31 (anti-CD31 antibody, 1:100, Santa cruz) immunofluorescence staining was performed on tumor tissue slices.

Immunofluorescence

When HUVECs grow to 80%~90% convergence on 14 mm cell crawls (Biosharp), cells were fixed with 4% paraformaldehyde and blocked with 5% BSA for 1 h. Then the cell climbing sheets were incubated overnight at 4 °C with the anti-rabbit-ZO-1 (1:200, CST). The secondary antibody

(1:1,000, Abcom) was bound at 37°C for 1 h and the nucleus was stained with Hoechst. Images were captured with a structured illumination microscopy (Nikon, SIM).

Transwell Migration and Invasion Assay of Tumor Cells

To verify whether GCMSC-CM treatment affected the recruitment ability of HUVECs to GC cells and the invasion ability of GC cells to cross the endothelial matrix, we constructed two Transwell experimental models. HUVECs were spread in the lower chamber of 24-well plates in advance and pretreated with GCMSC-CM for 24 h. 8×10^4 cells/200 μ L of HGC-27 and SGC-7901 were resuspended with serum-free 1640 and added to the upper chamber. The number of their migration to the lower chamber was detected after 8~10 h. To explore whether GCMSC-CM affected HUVECs' ability to recruit GC cells after the use of AKT inhibitors, Transwell migration experiments added MK-2206 (50 nM) along with GCMSC-CM treatment group, and other conditions remained the same. We diluted Recombinant Slit Homolog 2 (QCHENG BIO) to different concentrations (0 ng/ml, 100 ng/ml and 300 ng/ml) according to the instructions and added it to the lower layer of the culture medium containing 10% FBS to assess the effect of exogenous overexpression of Slit2 on the migration ability of SGC-7901, HGC-27 and HUVECs.

In the invasion experiment, HUVECs were spread in the upper chamber of Transwell 24-well plates in advance to form a single cell layer and pretreated with GCMSC-CM for 24 h. 6×10^4 cells/200 μ L of HGC-27-GFP and SGC-7901-GFP were resuspended with serum-free 1640 and added to the upper chamber. After 8 h, we used a cotton swab to remove the cells that did not migrate. Migrated cells were fixed with 4% formaldehyde for 30 min and then photographed and counted three random fields for each well under the microscope (Nikon).

Immunohistochemistry

In order to more visually localize the expression of Slit2 in different tumor sites of gastric cancer patients, immunohistochemical staining was performed. All patient slides were obtained from the Affiliated Hospital of Jiangsu University. Firstly, the tumor tissues, adjacent tissues and muscularis tissues were formalin fixed and embedded in paraffin, and then cut into 4 μ m sections. They were dewaxed in xylene, rehydrated with gradient ethanol, and treated with citrate buffer to extract antigens. The sections were incubated with anti-Slit2 antibody (rabbit, 1:200, Abcom) overnight at 4 °C and were then treated with polyperoxidase-conjugated IgG (OriGene). The samples stained with diaminobidine solution

(Biocare Medical) and counter-stained with haematoxylin were compared and photographed under a microscope.

qRT-PCR Analysis

TRIzol reagent (Ambion) was used to extract total RNA from HUVECs under different treatments with BMMSC-CM or GCMSC-CM. cDNA synthesis was processed by a reverse transcription kit according to the manufacturer's instructions (Cwbio). And then, qRT-PCR was performed in a reaction mixture according to the instructions. Primers employed were as follows: Slit2: forward, 5'-AGCCGAGG TTCAAAAACGAGA - 3', and reverse, 5'-GGCAGTGCA AAACACTACAAGA - 3'; GAPDH: forward, 5'-GGAGC GAGATCCCTCCAAAAT - 3', and reverse, 5'-GGCTGTT GTCATACTTCTCATGG - 3';

RNA Interference

Slit2 siRNA and negative control (NC) were purchased from RiboBio (Guangzhou, China). Cells transfection was performed according to the instructions. Briefly speaking, 1×10^5 cells/well HUVECs were seeded in a 6-well culture plate. siRNA and the negative control inhibitor were transfected into HUVECs with 6 μ L Lipofectamine® 2000 reagent (Invitrogen, Thermo Fisher Scientific Inc.) until the cell density reaches about 70%. The interference efficiency was verified by western blotting 12 h later.

Colony Formation Assay

HUVECs were pre-cultured with GCMSC-CM, MK-2206 (50 nM), or a combination of both for 24 h. 800 single cells of the three groups were seeded in 6-well plates in triplicate. When the number of cells in most cell colonies reaches 50~100, clonal formation is terminated. Cells were fixed with 4% paraformaldehyde and stained with 0.5% crystal violet solution (Sigma, USA) for 30 min. Colonies containing more than 50 cells were counted and photographed.

Statistical Analysis

Results were presented as mean \pm standard deviation (SD). Using GraphPad Prism software 6.0 (GraphPad Software, La Jolla, CA, USA) to analyze data. The independent t-test between two groups or one-way analysis of variance (ANOVA) were performed to analyze statistically with SPSS 16.0 statistical software, and *P*-value < 0.05 was considered statistically significant.

Results

GCMSC-CM Induced Functional Changes of HUVECs in Virto

CCK-8 assay showed that GCMSC-CM significantly increased cell proliferation of HUVECs at 72 h (Fig. 1A). Wound-healing assay and Transwell migration assay of HUVECs achieved the same result. After treatment with GCMSC-CM, the migration ability of endothelial cells was obviously enhanced (Fig. 1B, C). The stable increase in the expression of N-cadherin and Vimentin further suggests that GCMSC-CM may induce changes in the cytoskeleton

of HUVECs, leading to enhanced migration capability (Fig. 1D). Angiogenesis was detected after 4 h through tube formation assays. The number of branches and total branches lengths confirmed that GCMSC-CM, compared with the control group, promoted the proangiogenic activity of HUVECs (Fig. 1E). Coinciding with improved tube formation ability in vitro, vaso-specific marker CD31 was high expression in the tumor tissues of BALB/c nude mice after GCMSC-CM injected (Fig. 1F).

However, the observed upregulation of tight junctions' protein zonula occludens-1 (ZO-1) and E-cadherin may be attributed to the more pronounced impact of GCMSC-CM on the angiogenesis of HUVECs compared to its effect on

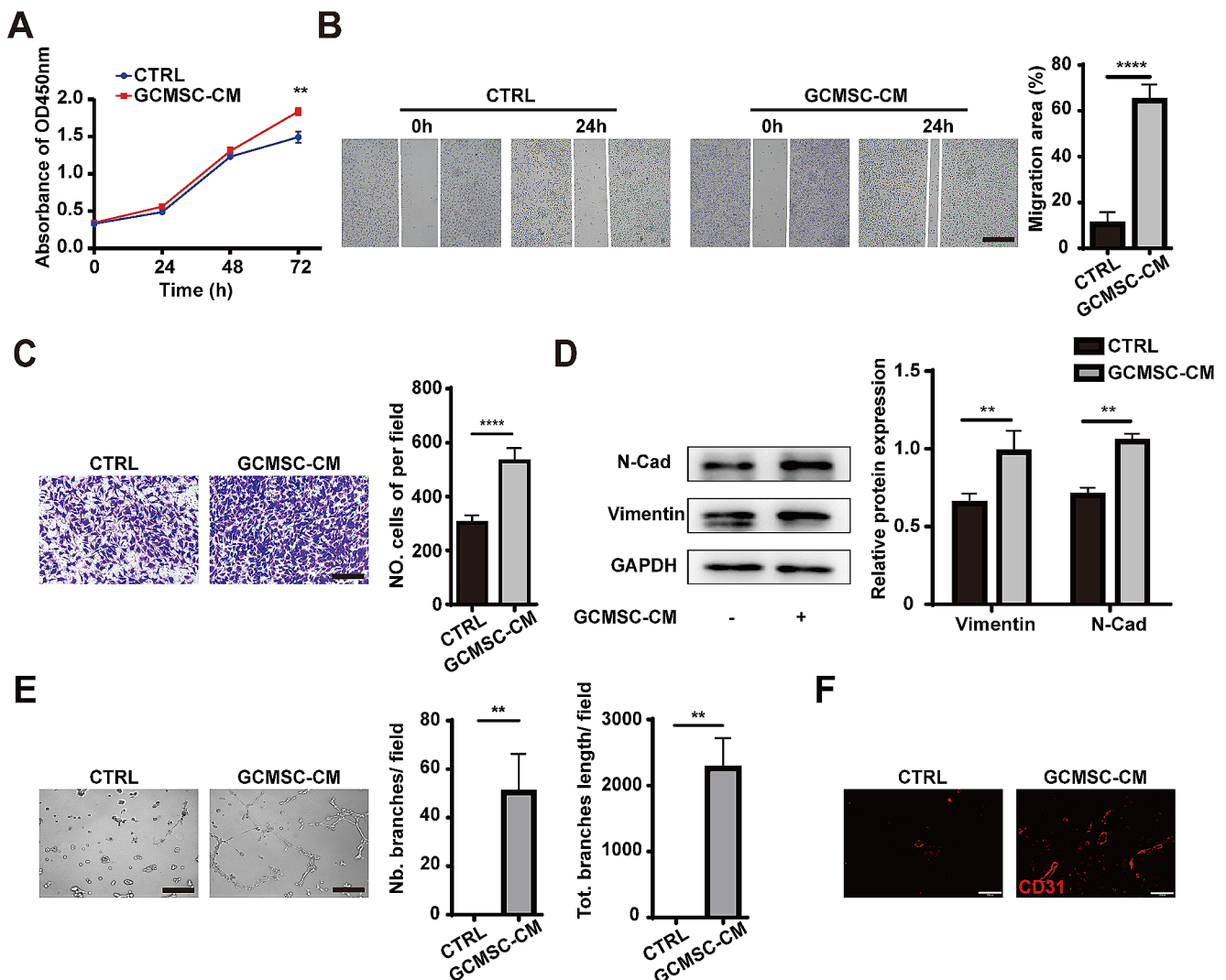


Fig. 1 GCMSC-CM induced functional changes in HUVECs in Virto. (A) Cell counting kit-8 assay (CCK-8) was used to detect the absorbance value at 450 nm of HUVECs after treatment with GCMSC-CM for 0 h, 24 h, 48 h and 72 h. (B–C) GCMSC-CM promoted HUVECs migration as analyzed by wound healing assay, scale bar: 250 μ m (B) and Transwell migration assay, scale bar: 100 μ m (C). (D) The expressions of N-cadherin and Vimentin in HUVECs were detected

and quantified. (E) GCMSC-CM increased the tube formation ability of HUVECs, Scale bar: 50 μ m. Quantitative analysis of branches numbers and total branch lengths were presented. (F) The vascular formation ability of BALB/c nude mice in tumor tissues was compared by CD31 immunofluorescence staining. Scale bar: 50 μ m. $n=4$ per group. **** $P < 0.0001$, *** $P < 0.001$, ** $P < 0.01$ and * $P < 0.05$

the disruption of vascular tight junctions. This could lead to an overall increase in the expression of both ZO-1 and E-cad (supplementary Fig. 1A–C).

Changes in HUVECs Function Led to Enhanced Migration and Invasion Ability of Tumor Cells

To evaluate the different recruitment ability to tumor cells of HUVECs, we established a gastric cancer cell migration model (Fig. 2A). The results showed that endothelial cells treated with GCMSC-CM showed stronger recruitment ability to HGC-27 and SGC-790 (Fig. 2B, C). Since tumor metastasis needs to penetrate vascular endothelial structure, we constructed an alternative model to examine trans endothelial invasion of cancer cells (HGC-27/SGC-7901/GFP) (Fig. 2D). There were significantly more GFP-labelled GC cells migrated through GCMSC-CM-treated HUVEC monolayer (Fig. 2E, F).

The Functional Changes of HUVECs Induced by GCMSC-CM may be Related to the Promotion of Slit2 Expression

In our previous studies, we observed that GCMSCs exhibit a greater propensity to enhance tumor progression within the tumor microenvironment compared to BMMSCs. In this

experiment, to further elucidate how GCMSCs induce functional alterations in HUVECs through the regulation of the pivotal protein Slit2, we compared the protein expression variations of Slit2 in HUVECs following treatment with BMMSC-CM and GCMSC-CM. Western blotting results showed that BMMSC-CM barely increased the protein expression of Slit2 (supplementary Fig. 2A). The quantitative statistics of the relative expression of mRNA showed more clearly that GCMSC-CM had a more important effect on HUVECs (supplementary Fig. 2B). We employed two different treatment methods for HUVECs. Western blotting analysis showed that GCMSCs supernatant treatment has a stronger effect than co-culture with GCMSCs (Fig. 3A). At 24 h and 36 h (Fig. 3B), the expression of Slit2 in HUVECs were increased more apparently. Therefore, we chose GCMSC-CM treatment for 24 h for the follow-up experiment.

Next, to verify that up-regulation of endothelial Slit2 expression promoted tumor metastasis, we used siRNA to interfere with Slit2 in HUVECs and verified the knock-down efficiency (Fig. 3C). According to the result, we chose siRNA fragment 2 for subsequent experiments. The results of the Transwell migration assay were consistent with our expectations. The recruitment ability of HUVECs to SGC-7901 was weakened compared with GCMSC-CM group and siSlit2+GCMSC-CM group (Fig. 3D). Furthermore,

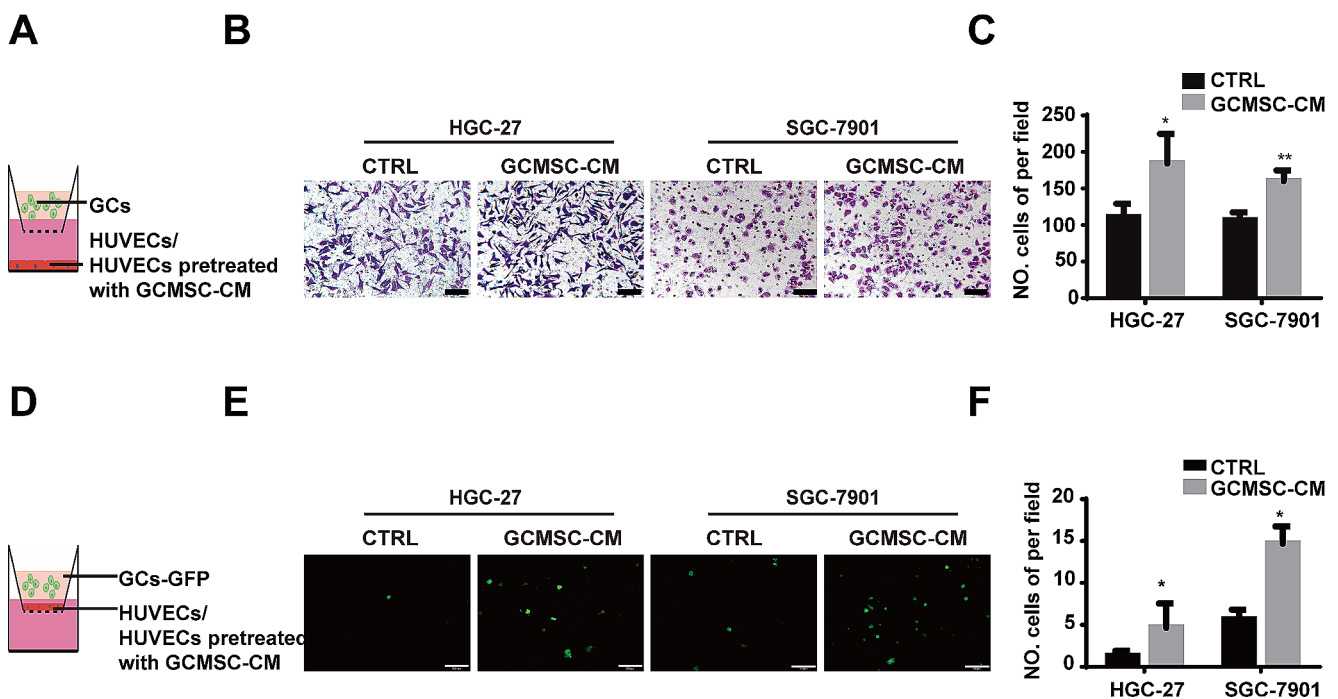
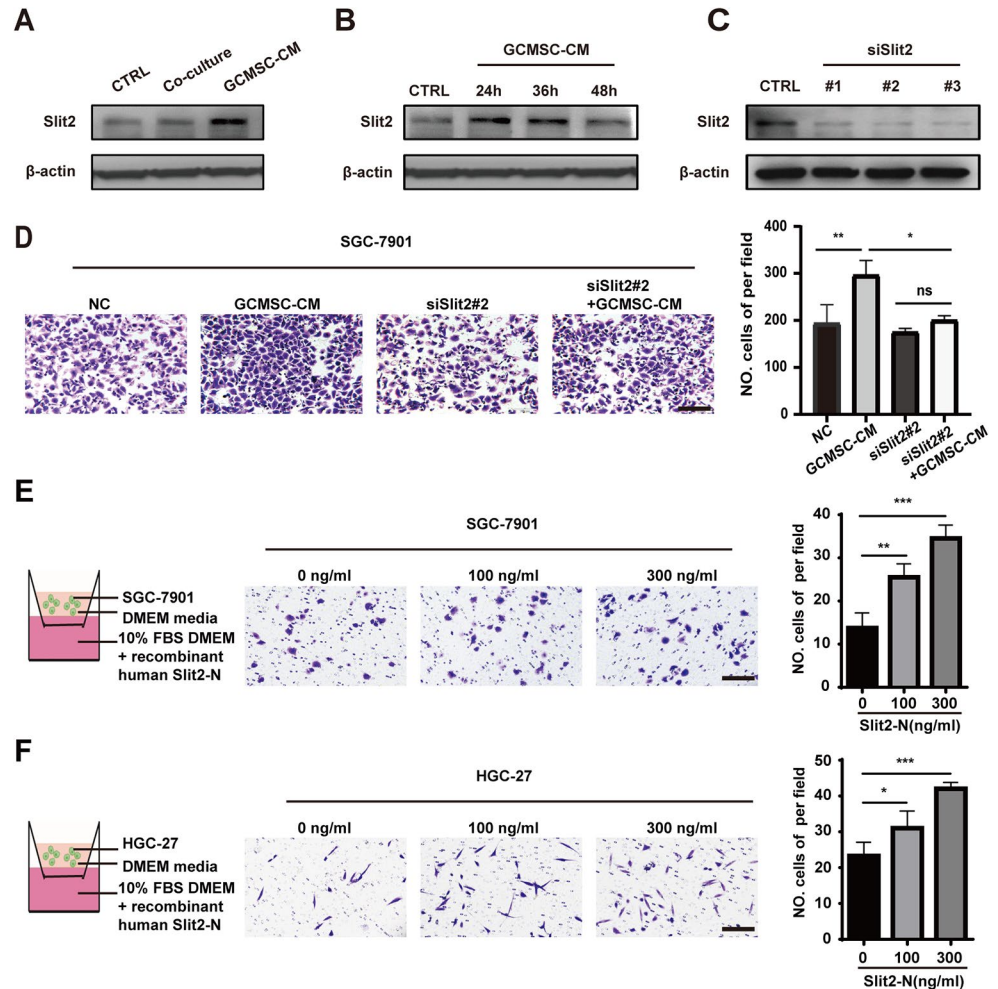


Fig. 2 The functional changes in HUVECs lead to enhanced migration and invasive capabilities of tumor cells. (A) Schematic illustration of HUVECs recruiting tumor cells. (B) Hematoxylin and eosin staining revealed the number of HGC-27 and SGC-7901 recruited by HUVECs in four different fields. Scar bar: 50 μ m. (C) Quantitative plot

of recruited cells. $n=4$ per group. (D) Model diagram of tumor cell infiltration into a monolayer of HUVECs. (E) HGC-27 or SGC-7901 labeled with GFP penetrating through the endothelial cell layer were detected. Scar bar: 50 μ m. (F) Quantitative plot of invasive cells. $n=4$ per group. **** $P < 0.0001$, *** $P < 0.001$, ** $P < 0.01$ and * $P < 0.05$

Fig. 3 GCMSCs up-regulate the expression of Slit2 in endothelial cells and promote tumor migration. **(A)** The expression of Slit2 in HUVECs co-cultured with GCMSCs or treated with GCMSC-CM was detected by western blotting. **(B)** Slit2 expression was detected by western blotting after GCMSC-CM treatment for 24 h, 36 h and 48 h. **(C)** The efficiency of Slit2 knock-down by siRNA in HUVECs was verified. **(D)** Transwell migration assay was employed to assess the ability of HUVECs to recruit SGC-7901 cell. $n=3$. **(E-F)** Schematic diagram and staining results of SGC-7901 **(E)** and HGC-27 **(F)** recruited using different concentrations of human recombinant protein Slit2-N (0 ng/ml, 100 ng/ml, 300 ng/ml), and the number of migrating cells was quantified. Scar bar: 50 μ m. $n=3$ per group. **** $P < 0.0001$, *** $P < 0.001$, ** $P < 0.01$ and * $P < 0.05$



we utilized recombinant human Slit2-N protein standard to overexpress exogenous Slit2. The results demonstrated that both 100ng/ml and 300ng/ml concentrations promoted the migration of SGC-7901 and HGC-27 cells, showing a dose-dependent effect (Fig. 3E, F). These results suggested that GCMSCs may promote GC cells migration by upregulating the expression of Slit2 in endothelial cells.

Slit2 is Positively Correlated with the Expression of Mesenchymal Stem-Related Factors

We used SangerBox [31] to further verify the correlation factors that interact with Slit2 in gastric cancer, including vascular-related factors, tumor related factors, and perivascular stem-related factors (Fig. 4A). Specifically, Slit2 was positively correlated with the expression of vascular endothelial signature factor (VWF + PECAM1) (Fig. 4B), lymphatic endothelial factor (LYVE1 + PECAM1) (Fig. 4C) and perivascular mesenchymal stem signature factor (MUC1 + MUC2 + KRT18 + KRT19) (Fig. 4D). It was negatively correlated with the expression of tumor related factors (THY1 + ENG + NT5E + VCAM1) (Fig. 4E).

GCMSC-CM may Promote Slit2 Expression by Regulating AKT Phosphorylation, Leading to Functional and Recruitment Ability to Tumor Cells Changes in HUVECs

Western blotting results showed that the expression of phosphorylated AKT protein increased after GCMSC-CM treatment (Fig. 5A). Then, we used MK-2206 (50nM) to inhibit AKT phosphorylation. At the same time, we observed inhibition in the expression of Slit2 when phosphorylated AKT expression was suppressed (Fig. 5B). The application of MK-2206 reversed the increase in N-cad and E-cad expression induced by GCMSC-CM (Fig. 5C and supplementary Fig. 3A). We repeated the previous experiments on endothelial cell migration ability. The results also demonstrated that the use of p-AKT inhibitors attenuated the enhancement in HUVECs' migration induced by GCMSC-CM (Fig. 5D, E). In addition, we also employed overexpressed Slit2-N recombinant protein to recruit HUVECs in vitro. The results showed enhanced migration ability of HUVECs. This provides further evidence that GCMSCs

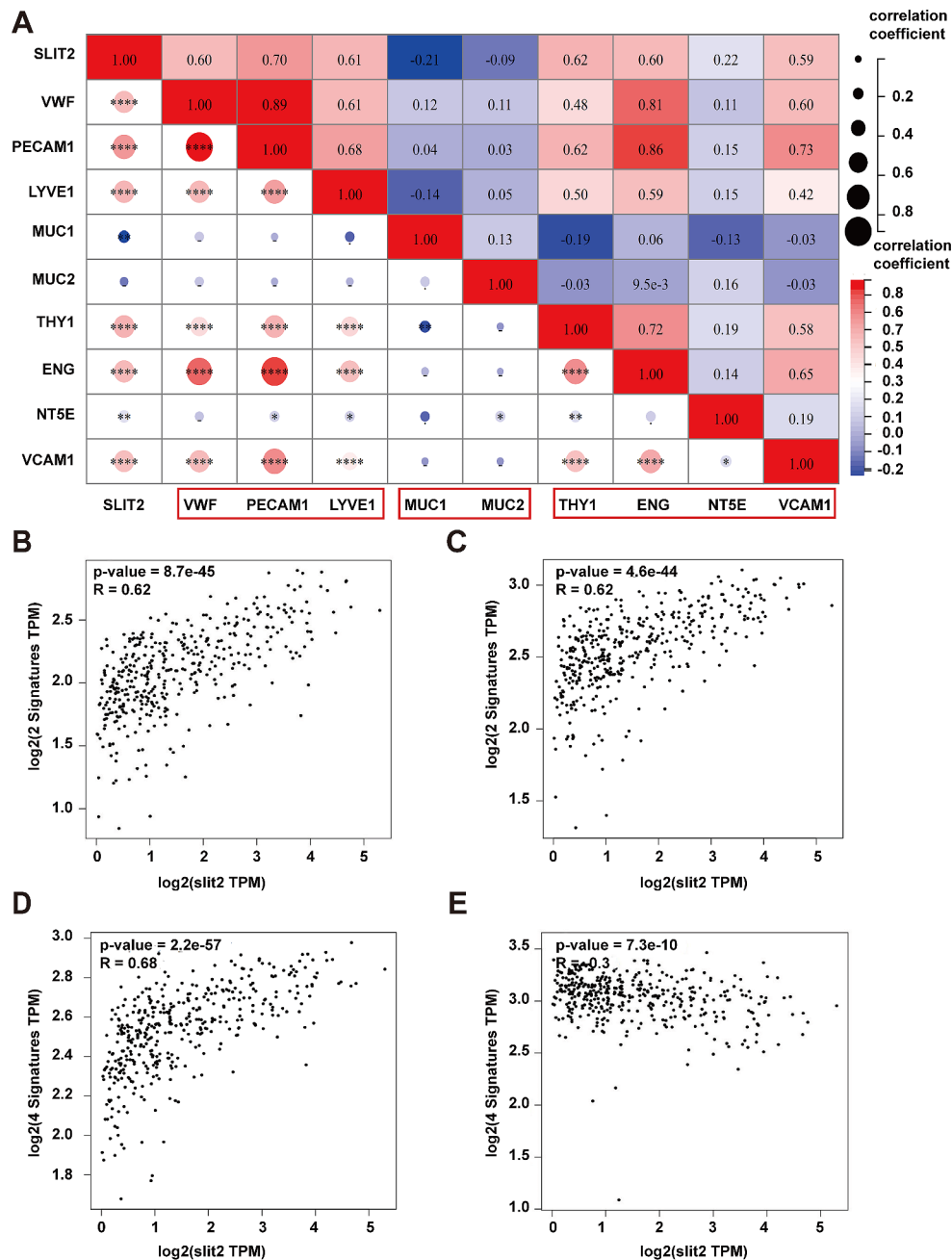


Fig. 4 The correlation factors interacting with Slit2. **(A)** Correlation between vascular-related factors, tumor related factors, perivascular stem-related factors and Slit2 expression. **(B)** Correlation between VWF+PECAM1 and Slit2. **(C)** Correlation

between LYVE1+PECAM1 and Slit2. **(D)** Correlation between MUC1+MUC2+KRT18+KRT19 and Slit2. **(E)** Correlation between THY1+ENG+NT5E+VCAM1 and Slit2

may influence cellular function by promoting the expression levels of Slit2 in HUVECs (supplementary Fig. 3B). The suppression of AKT signal also partially reduced the promotion on the proliferation of HUVECs cells (Fig. 5F). Similarly, Transwell migration assays were employed to assess alterations in the recruitment ability of HUVECs to GC cells following MK-2206 application. It was observed that the impact of GCMSC-CM was diminished upon AKT

signaling inhibition in both HGC-27 and SGC-7901 cells (Fig. 5G, H).

The Expression of Slit2 is Higher in the Tumor Tissues of Gastric Cancer Patients

We observed that higher Slit2 expression was associated with poorer survival outcomes from GEPIA 2.0 database

Fig. 5 Inhibiting AKT phosphorylation can partially suppress the functional changes and recruitment abilities to GC cells in HUVECs induced by GCMSC-CM. **(A)** The protein expression changes of total AKT and phosphorylated AKT were detected by western blotting. **(B)** Slit2 expression was analyzed following p-AKT inhibition with MK-2206 (50 nM). **(C)** The use of MK-2206 (50 nM) can reduce the expression of N-Cad in HUVECs. **(D-E)** Wound healing experiments **(D)** and Transwell migration assays **(E)** were conducted to assess the impact of inhibiting p-AKT on the migration ability of HUVECs induced by GCMSC-CM. Scale bar: 250 μ m and 50 μ m respectively. **(F)** Colony formation assay demonstrated the effects of GCMSC-CM and MK-2206 (50 nM) on the proliferative capacity of HUVECs. **(G-H)** Transwell migration assay revealed the number of HGC-27 **(G)** and SGC-7901 **(H)** recruited by HUVECs in four different fields. Scale bar: 50 μ m. $n = 3$ per group. **** $P < 0.0001$, *** $P < 0.001$, ** $P < 0.01$ and * $P < 0.05$

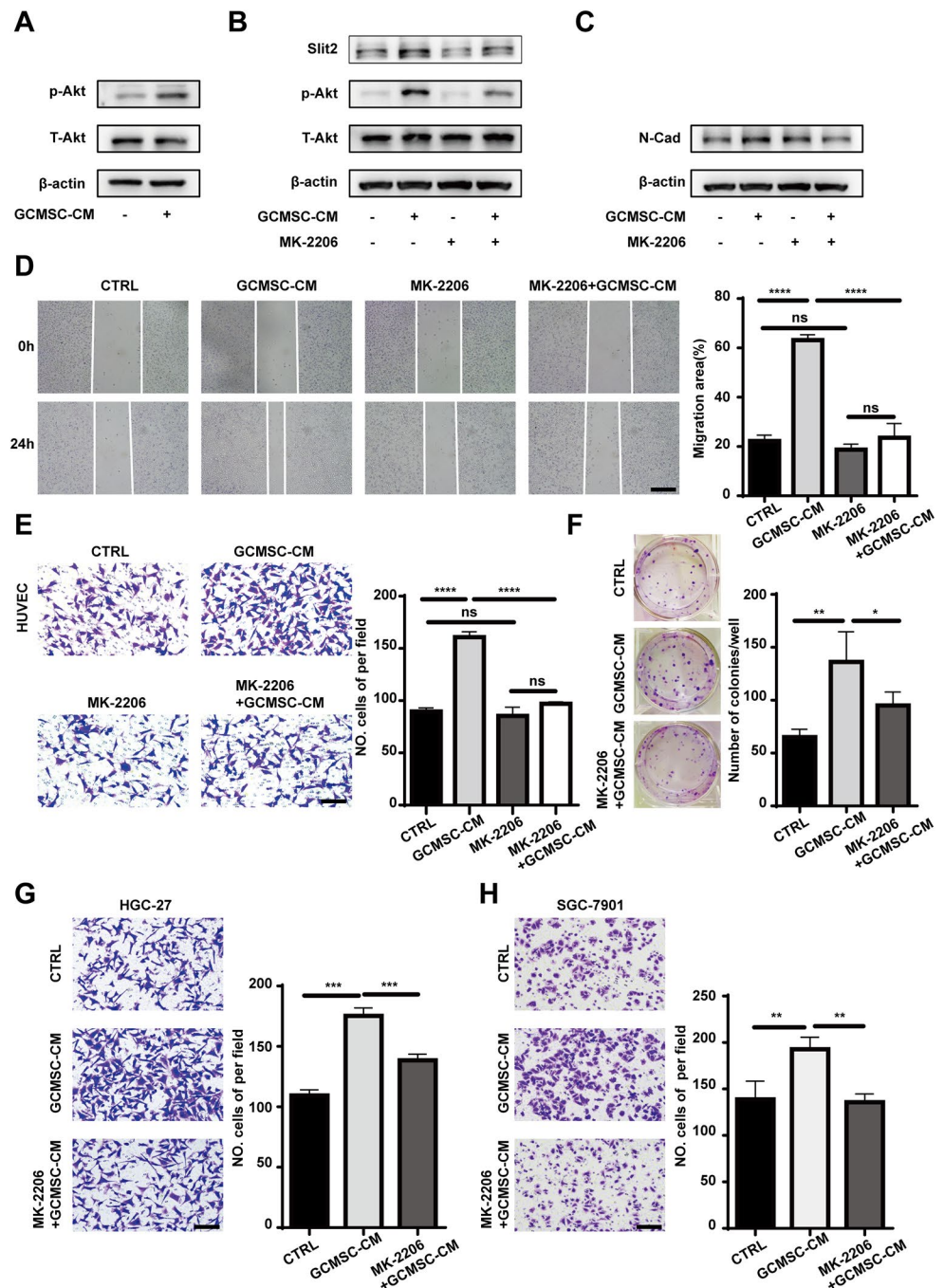


(Fig. 6A, B). Higher Slit2 expression positively correlated with advanced GC stage and shorter overall survival of patients. Next, we proceeded to further investigate the expression of Slit2 in gastric cancer patients in vivo. We investigated the expression and localization of Slit2 in GC tissues, para-cancerous tissues, and muscular tissues. As depicted in Fig. 6C, a higher abundance of Slit2 proteins was observed in proximity to blood vessels within tumor tissues.

Discussion

Several studies have consistently demonstrated that high angiogenic activity in endothelial cells is closely linked to advanced metastasis and recurrence in human cancers [26]. The process of tumor metastasis typically involves tumor cells initially invading the extracellular matrix [32], followed by their entry into the bloodstream through vascular endothelial cells with compromised tight junctions. Ultimately, these tumor cells disseminate to distant organs or

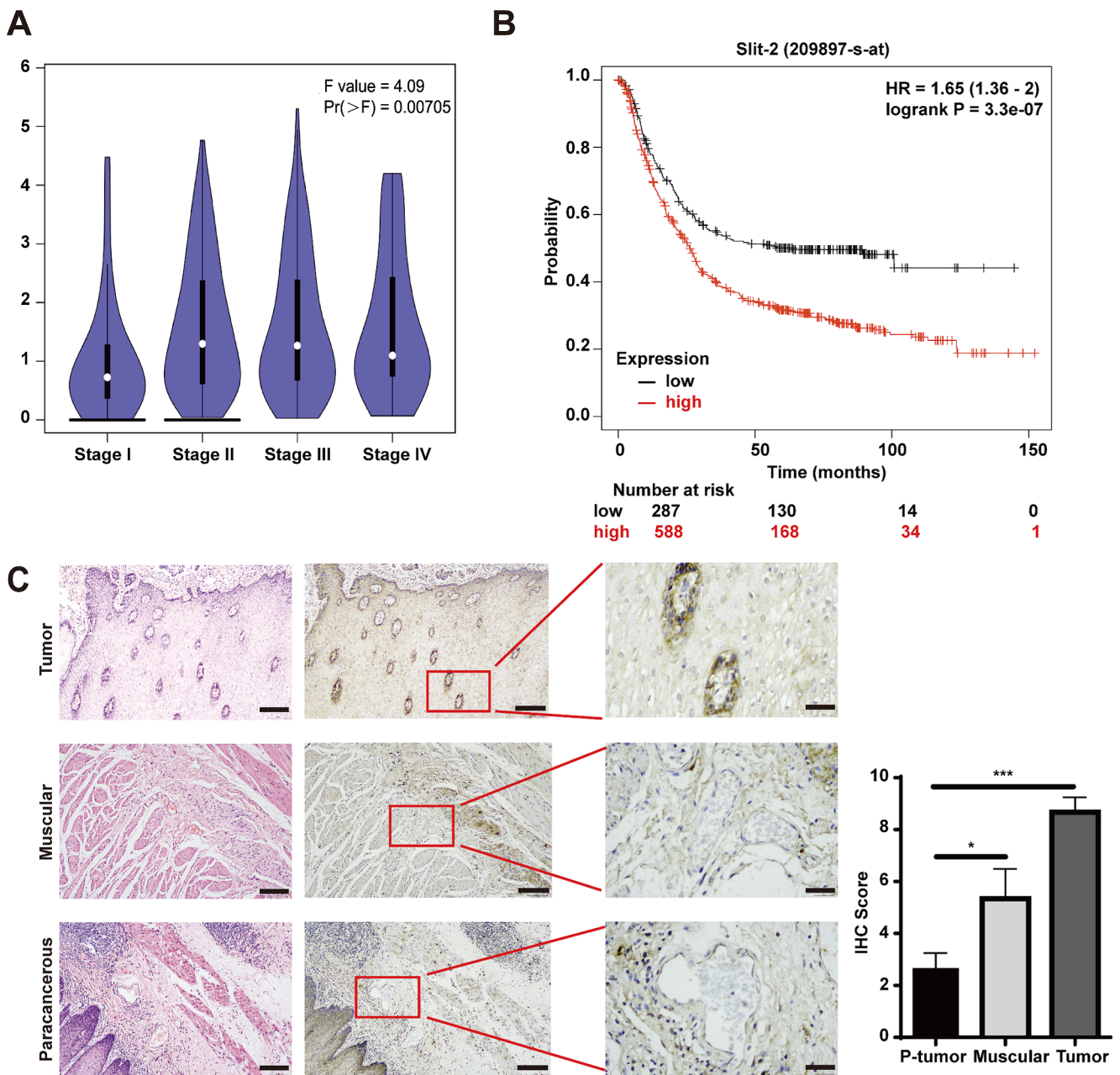


Fig. 6 The expression and localization patterns of Slit2 in gastric cancer patients. **(A)** GEPIA 2.0 database was used to analyze the expression of Slit2 in different stages of gastric cancer. **(B)** Kaplan-Meier analysis of overall survival for patients with GC based on Slit2 expres-

sion. **(C)** HE staining (left) and immunohistochemical staining were used to detect the expression and localization of Slit2 in gastric cancer. The staining results were analyzed quantitatively by pathological scores. $n = 3$ per group. Scale bar: 50 μm (left). Scale bar: 10 μm (right)

tissues via the bloodstream [33]. Throughout this process, the tumor microenvironment plays a pivotal role [34]. As a significant stromal component within the tumor microenvironment, GCMSCs have been reported to possess immunosuppressive functions and are also implicated in tumor angiogenesis and the remodeling of the extracellular matrix. However, it remains unclear whether there exists a correlation between GCMSCs and the promotion of gastric cancer

progression mediated by endothelial cells. In this study, we aimed to investigate the interplay between GCMSCs and HUVECs in the context of promoting gastric cancer progression and explore the potential underlying mechanisms.

It has been well-documented that endothelial cell proliferation, migration [35], and angiogenic capacity [26] are fundamental prerequisites for tumor progression and metastasis [36]. In our study, we exposed HUVECs to

GCMSC-CM and examined its impact on the proliferation and migration of HUVECs. Our findings revealed an enhancement in both of them. Furthermore, *in vitro* tube formation assays demonstrated that HUVECs treated with GCMSC-CM exhibited a more robust angiogenic capacity, which was in line with the outcomes of vascular formation assays conducted in BALB/c subcutaneous tumor-bearing nude mice. These results were further corroborated by Western blotting analysis. The increased expression of N-cad and Vimentin suggested that endothelial cells may acquire fibroblast-like characteristics, experience a loss of tight intercellular connections, and exhibit disruption in the vascular wall structure [37, 38].

Previous research has consistently observed that mesenchymal stem cells within TME can indeed facilitate tumor metastasis [39]. To delve deeper into whether GCMSCs promote tumor metastasis through their interactions with ECs, we optimized an *in vitro* tumor metastasis model based on prior research [40]. The results from Transwell experiments revealed a significant enhancement in HUVECs' ability to recruit GC cells and GC cells' ability to traverse the HUVECs' extracellular matrix after treatment with GCMSC-CM. These findings substantiate our hypothesis that GCMSCs can exert their influence on HUVECs to facilitate gastric cancer metastasis. The underlying mechanism is waiting for further investigations.

The role of the secreted protein Slit2, expressed by vascular endothelial cells, has been extensively investigated. Slit2 is known to regulate the migration and osmotic activity of endothelial cells by binding to its receptor Robo [41, 42]. Also, Slit2 has been shown to promote vascular infiltration and the migration of cancer cells into endothelial cells [40, 43]. Analyses from the GEPIA 2.0 database indicated that Slit2 expression in gastric adenocarcinoma correlates with the progression and prognosis of gastric cancer.

In our study, we aimed to examine the expression of Slit2 in HUVECs treated with GCMSC-CM or co-cultured with GCMSCs. The results indicated that compared to coculturing HUVECs with GCMSCs for 24 h, direct treatment with GCMSC-CM for 24 h significantly upregulated the expression of Slit2. This observation could be attributed to the interplay between the two cell types during coculture, where the number of GCMSCs seeded in the well was notably lower than that of HUVECs, potentially resulting in HUVECs suppressing the secretion of certain cytokines by GCMSCs. Alternatively, the shorter duration of coculture might mask the effect of GCMSCs on augmenting Slit2 protein levels in HUVECs. Remarkably, BMMSCs did not elicit a similar effect, indicating that certain soluble factors secreted by GCMSCs in the supernatant might be responsible.

To further elucidate this mechanism, we conducted Slit2 knockdown experiments in HUVECs, revealing a reduction in the recruitment ability of HUVECs to GC cells. Additionally, we observed enhanced migration ability of tumor cells upon treatment with overexpressed Slit2-N recombinant protein, demonstrating a dose-dependent effect. These findings provide additional evidence supporting the hypothesis that GCMSCs may promote tumor progression by upregulating the expression of Slit2 in endothelial cells.

Furthermore, we employed SangerBox to predict the factors that interact with Slit2 and found differences in four distinct aspects. The outcomes revealed a positive correlation between the expression of Slit2 and vascular-related factors. Consistent with our experimental expectations, the expression of Slit2 also exhibited a positive correlation with mesenchymal stem-related markers.

Finally, our aim was to unravel the pathway by which GCMSC-CM influences the expression of Slit2 protein in endothelial cells, subsequently impacting the cellular functions of HUVECs. It has been reported that the PI3K/AKT signaling pathway can modulate endothelial cell tube formation and tumor progression [26, 44]. Therefore, we evaluated the expression of AKT protein following treatment with the GCMSC-CM. The results demonstrated a significant upregulation of p-AKT protein expression. To further establish the link, we utilized the phosphorylated AKT inhibitor to demonstrate that AKT signaling indeed regulates Slit2 expression in endothelial cells. Additionally, the expression of N-cad was also found to be inhibited. Consistent conclusions were obtained that inhibition of the AKT signaling pathway could partially counteract the functional changes of HUVECs and the recruitment ability to GC cells.

Our research team previously employed gene chip technology to screen for differential cell factors between BMMSC-CM and GCMSC-CM, revealing that the expression levels of IL-6, IL-8, HGF, CCL11, MCP2, MCP3, and MIF were higher in GCMSC-CM compared to BMMSC-CM [8]. These potential cell factors may induce phosphorylation changes in AKT. Furthermore, further studies have found a potential link between the tumor microenvironment immunotolerance mediated by GCMSCs and AKT phosphorylation mediated by IL-8 derived from GCMSCs [29]. These findings have given us confidence that the highly expressed soluble cell factors in GCMSC-CM may induce changes in endothelial cell function through the IL-8/Slit2/PI3K/p-AKT/mTOR pathway, thereby promoting gastric cancer progression. In future research, we plan to use IL-8 neutralizing antibodies to neutralize IL-8 in GCMSC-CM and continue to explore the downstream signaling molecules of Slit2, refine the regulatory pathways of GCMSC-CM on HUVECs, and validate them in *in vivo* experiments.

In summary, this study highlights that GCMSCs supernatant upregulates Slit2 expression in endothelial cells by modulating AKT phosphorylation, leading to functional alterations in HUVECs. These changes include enhanced endothelial cell proliferation and migration, along with increased angiogenesis capabilities, ultimately creating more vessels for tumor cells. On the other hand, the disruption of the tight intercellular connections among endothelial cells and the compromise of blood vessel integrity further facilitates tumor cell infiltration and dissemination to new sites via the bloodstream. This cascade of events that together promote cancer progression. Overall, GCMSCs promote the progression of gastric cancer through two mechanisms: enhancing angiogenesis within the tumor microenvironment and disrupting the tight connections between endothelial cells.

Conclusion

In conclusion, this investigation revealed that GCMSCs could potentially influence Slit2 expression in endothelial cells through the AKT signaling pathway, resulting in functional alterations in ECs that contribute to tumor progression. These findings not only offer new insights into the mechanisms underlying GCMSC-mediated gastric cancer progression but also present a potential strategy to enhance the effectiveness of immunotherapy.

Supplementary Information The online version contains supplementary material available at <https://doi.org/10.1007/s12015-024-10720-8>.

Acknowledgements The authors would like to further acknowledge the financial support from the National Natural Science Foundation of China, Medical Research project of Jiangsu Provincial Health Commission and Jiangsu National Natural Science Foundation. The authors would also like to express our gratitude for the drawing materials provided by BioRender.

Author Contributions LC: Generated experimental data, Manuscript writing, experimental design; TL: Generated experimental data, experimental design; CH: Generated experimental data, experimental design; FY: Experimental data generation, experimental design; LL: Experimental data generation, experimental design; LS: Experimental data generation, samples collection; YZ: Experimental data generation, samples collection; DW: Experimental design, manuscript editing; MW: Experimental design, manuscript revision; YJ: Experimental design, manuscript revision; WZ: Experimental design, manuscript revision.

Funding This work was supported by the National Natural Science Foundation of China (Grant numbers 81972313 and 82203547); Medical Research project of Jiangsu Provincial Health Commission (Grant number X373); and Jiangsu National Natural Science Foundation (Grant number BK20210136).

Data Availability The data that support the findings of this study are available from the corresponding author upon reasonable request.

Code Availability Not applicable.

Declarations

Ethical Approval All studies were conducted in accordance with the Ethics Committee of Jiangsu University and informed consent was obtained from all subjects.

Consent to Participate Informed consent was obtained from all individual participants included in the study.

Consent for Publication The authors affirm that all participants provided informed consent for publication of the paper.

Conflict of Interest The authors have no relevant financial or non-financial interests to disclose.

References

- Zheng, R., Zhang, S., Zeng, H., Wang, S., Sun, K., Chen, R., Li, L., Wei, W., & He, J. (2022). Cancer incidence and mortality in China, 2016. *Journal of the National Cancer Center*.
- Quail, D., & Joyce, J. (2013). Microenvironmental regulation of tumor progression and metastasis. *Nature Medicine*, 19(11), 1423–1437. <https://doi.org/10.1038/nm.3394>.
- Rankin, E., & Giaccia, A. (2016). Hypoxic control of metastasis. *Science (New York N Y)*, 352(6282), 175–180. <https://doi.org/10.1126/science.aaf4405>.
- Pitt, J., Marabelle, A., Eggermont, A., Soria, J., Kroemer, G., & Zitvogel, L. (2016). Targeting the tumor microenvironment: Removing obstruction to anticancer immune responses and immunotherapy. *Annals of Oncology: Official Journal of the European Society for Medical Oncology*, 27(8), 1482–1492. <https://doi.org/10.1093/annonc/mdw168>.
- Yang, L., Ping, Y., Yu, X., Qian, F., Guo, Z., Qian, C., Cui, Y., & Bian, X. (2011). Gastric cancer stem-like cells possess higher capability of invasion and metastasis in association with a mesenchymal transition phenotype. *Cancer Letters*, 310(1), 46–52. <https://doi.org/10.1016/j.canlet.2011.06.003>.
- Quante, M., Tu, S., Tomita, H., Gonda, T., Wang, S., Takashi, S., Baik, G., Shibata, W., Diprete, B., Betz, K., Friedman, R., Varro, A., Tycko, B., & Wang, T. (2011). Bone marrow-derived myofibroblasts contribute to the mesenchymal stem cell niche and promote tumor growth. *Cancer Cell*, 19(2), 257–272. <https://doi.org/10.1016/j.ccr.2011.01.020>.
- Cao, H., Xu, W., Qian, H., Zhu, W., Yan, Y., Zhou, H., Zhang, X., Xu, X., Li, J., Chen, Z., & Xu, X. (2009). Mesenchymal stem cell-like cells derived from human gastric cancer tissues. *Cancer Letters*, 274(1), 61–71. <https://doi.org/10.1016/j.canlet.2008.08.036>.
- Sun, L., Wang, Q., Chen, B., Zhao, Y., Shen, B., Wang, H., Xu, J., Zhu, M., Zhao, X., Xu, C., Chen, Z., Wang, M., Xu, W., & Zhu, W. (2018). Gastric cancer mesenchymal stem cells derived IL-8 induces PD-L1 expression in gastric cancer cells via STAT3/mTOR-c-Myc signal axis. *Cell Death & Disease*, 9(9), 928. <https://doi.org/10.1038/s41419-018-0988-9>.
- Li, W., Zhang, X., Wu, F., Zhou, Y., Bao, Z., Li, H., Zheng, P., & Zhao, S. (2019). Dec 4). Gastric cancer-derived mesenchymal stromal cells trigger M2 macrophage polarization that promotes

- metastasis and EMT in gastric cancer. *Cell Death and Disease*, 10(12), 918. <https://doi.org/10.1038/s41419-019-2131-y>.
10. Shen, J., & Zhu, W. (2021). Research advances in the role of gastric cancer-derived mesenchymal stem cells in tumor progression (review). *International Journal of Molecular Medicine*, 47(2), 455–462. <https://doi.org/10.3892/ijmm.2020.4810>.
 11. Wan, L., Pantel, K., & Kang, Y. (2013). Tumor metastasis: Moving new biological insights into the clinic. *Nature Medicine*, 19(11), 1450–1464. <https://doi.org/10.1038/nm.3391>.
 12. Dammeijer, F., van Gulijk, M., Mulder, E., Lukkes, M., Klaase, L., van den Bosch, T., van Nimwegen, M., Lau, S., Latupeirissa, K., Schetters, S., van Kooyk, Y., Boon, L., Moyaart, A., Mueller, Y., Katsikis, P., Eggermont, A., Vroman, H., Stadhouders, R., Hendriks, R., Thüsen, J., Grünhagen, D., Verhoef, C., van Hall, T., & Aerts, J. (2020). The PD-1/PD-L1-Checkpoint restrains T cell immunity in Tumor-Draining Lymph Nodes. *Cancer Cell*, 38(5), 685–700e688. <https://doi.org/10.1016/j.ccell.2020.09.001>.
 13. Pradeep, S., Kim, S., Wu, S., Nishimura, M., Chaluvally-Raghavan, P., Miyake, T., Pecot, C., Kim, S., Choi, H., Bischoff, F., Mayer, J., Huang, L., Nick, A., Hall, C., Rodriguez-Aguayo, C., Zand, B., Dalton, H., Arumugam, T., Lee, H., Han, H., Cho, M., Rupaimoole, R., Mangala, L., Sehgal, V., Oh, S., Liu, J., Lee, J., Coleman, R., Ram, P., Lopez-Berestein, G., Fidler, I., & Sood, A. (2014). Hematogenous metastasis of ovarian cancer: Rethinking mode of spread. *Cancer Cell*, 26(1), 77–91. <https://doi.org/10.1016/j.ccr.2014.05.002>.
 14. Sturtzel, C. (2017). Endothelial cells. *Advances in Experimental Medicine and Biology*, 1003, 71–91. https://doi.org/10.1007/978-3-319-57613-8_4.
 15. Gaikwad, A. V., Eapen, M. S., McAlinden, K. D., Chia, C., Larby, J., Myers, S., Dey, S., Haug, G., Markos, J., Glanville, A. R., & Sohal, S. S. (2020, Oct). Endothelial to mesenchymal transition (EndMT) and vascular remodeling in pulmonary hypertension and idiopathic pulmonary fibrosis. *Expert Review of Respiratory Medicine*, 14(10), 1027–1043. <https://doi.org/10.1080/17476348.2020.1795832>.
 16. Huang, H., Chen, L., Sun, W., Du, H., Dong, S., Ahmed, A., Cao, D., Cui, J., Zhang, Y., & Cao, Q. (2021). Collagenase IV and clusterin-modified polycaprolactone-polyethylene glycol nanoparticles for penetrating dense tumor tissues. *Theranostics*, 11(2), 906–924. <https://doi.org/10.7150/thno.47446>.
 17. Seoane, J., & Gomis, R. (2017). TGF- β Family Signaling in Tumor suppression and Cancer progression. *Cold Spring Harbor Perspectives in Biology*, 9(12). <https://doi.org/10.1101/cshperspect.a022277>.
 18. Kaushik, N., Kim, S., Suh, Y., & Lee, S. (2019). Proinvasive extracellular matrix remodeling for tumor progression. *Archives of Pharmacol Research*, 42(1), 40–47. <https://doi.org/10.1007/s12272-018-1097-0>.
 19. Shu, D. Y., Butcher, E., & Saint-Geniez, M. (2020, Jun 16). EMT and EndMT: Emerging roles in age-related Macular Degeneration. *International Journal of Molecular Sciences*, 21(12). <https://doi.org/10.3390/ijms21124271>.
 20. Xu-Dubois, Y., Peltier, J., Brocheriou, I., Suberbielle-Boissel, C., Djamali, A., Reese, S., Mooney, N., Keuylian, Z., Lion, J., Ouali, N., Levy, P., Jouanneau, C., Rondeau, E., & Hertig, A. (2016). Markers of endothelial-to-mesenchymal transition: Evidence for antibody-endothelium Interaction during antibody-mediated rejection in kidney recipients. *Journal of the American Society of Nephrology: JASN*, 27(1), 324–332. <https://doi.org/10.1681/asn.2014070679>.
 21. Zhang, L., He, J., Wang, J., Liu, J., Chen, Z., Deng, B., Wei, L., Wu, H., Liang, B., Li, H., Huang, Y., Lu, L., Yang, Z., Xian, S., & Wang, L. (2021). Knockout RAGE alleviates cardiac fibrosis through repressing endothelial-to-mesenchymal transition (EndMT) mediated by autophagy. *Cell Death & Disease*, 12(5), 470. <https://doi.org/10.1038/s41419-021-03750-4>.
 22. Xu, Z., Guo, C., Ye, Q., Shi, Y., Sun, Y., Zhang, J., Huang, J., Huang, Y., Zeng, C., Zhang, X., Ke, Y., & Cheng, H. (2021). Endothelial deletion of SHP2 suppresses tumor angiogenesis and promotes vascular normalization. *Nature Communications*, 12(1). <https://doi.org/10.1038/s41467-021-26697-8>.
 23. Shoemaker, L. D., McCormick, A. K., Allen, B. M., & Chang, S. D. (2020, Jun). Evidence for endothelial-to-mesenchymal transition in human brain arteriovenous malformations. *Clin Transl Med*, 10(2), e99. <https://doi.org/10.1002/ctm2.99>.
 24. Liang, G., Wang, S., Shao, J., Jin, Y., Xu, L., Yan, Y., Günther, S., Wang, L., & Offermanns, S. (2022). Tenascin-X mediates Flow-Induced suppression of EndMT and atherosclerosis. *Circulation Research*, 130(11), 1647–1659. <https://doi.org/10.1161/circresaha.121.320694>.
 25. Wang, X., Chen, Z., Xu, J., Tang, S., An, N., Jiang, L., Zhang, Y., Zhang, S., Zhang, Q., Shen, Y., Chen, S., Lan, X., Wang, T., Zhai, L., Cao, S., Guo, S., Liu, Y., Bi, A., Chen, Y., Gai, X., Duan, Y., Zheng, Y., Fu, Y., Li, Y., Yuan, L., Tong, L., Mo, K., Wang, M., Lin, S., Tan, M., Luo, C., Chen, Y., Liu, J., Zhang, Q., Li, L., & Huang, M. (2022). SLC1A1-mediated cellular and mitochondrial influx of R-2-hydroxyglutarate in vascular endothelial cells promotes tumor angiogenesis in IDH1-mutant solid tumors. *Cell Research*, 32(7), 638–658. <https://doi.org/10.1038/s41422-022-00650-w>.
 26. Cheng, H., Chen, Y., Wong, J., Weng, C., Chen, H., Yu, S., Chen, H., Yuan, A., & Chen, J. (2017). Cancer cells increase endothelial cell tube formation and survival by activating the PI3K/Akt signalling pathway. *Journal of Experimental & Clinical Cancer Research: CR*, 36(1), 27. <https://doi.org/10.1186/s13046-017-0495-3>.
 27. Romano, E., Manetti, M., Rosa, I., Fioretto, B., Ibba-Manneschi, L., Matucci-Cerinic, M., & Guiducci, S. (2018). Slit2/Robo4 axis may contribute to endothelial cell dysfunction and angiogenesis disturbance in systemic sclerosis. *Annals of the Rheumatic Diseases*, 77(11), 1665–1674. <https://doi.org/10.1136/annrheumdis-2018-213239>.
 28. Lu, L., Li, X., Zhong, Z., Zhou, W., Zhou, D., Zhu, M., & Miao, C. (2021). KMT5A downregulation participated in high glucose-mediated EndMT via Upregulation of ENO1 expression in Diabetic Nephropathy. *International Journal of Biological Sciences*, 17(15), 4093–4107. <https://doi.org/10.7150/ijbs.62867>.
 29. Huang, C., Chen, B., Wang, X., Xu, J., Sun, L., Wang, D., Zhao, Y., Zhou, C., Gao, Q., Wang, Q., Chen, Z., Wang, M., Zhang, X., Xu, W., Shen, B., & Zhu, W. (2023). Gastric cancer mesenchymal stem cells via the CXCR2/HK2/PD-L1 pathway mediate immunosuppression. *Gastric cancer: Official Journal of the International Gastric Cancer Association and the Japanese Gastric Cancer Association*, 26(5), 691–707. <https://doi.org/10.1007/s10120-023-01405-1>.
 30. Han, F., Guo, S., Huang, C., Cui, L., Zhao, Y., Ma, J., Zhu, M., Chen, Z., Wang, M., Shen, B., & Zhu, W. (2021). Gastric cancer mesenchymal stem cells inhibit natural killer cell function by up-regulating FBP1. *Central-European Journal of Immunology*, 46(4), 427–437. <https://doi.org/10.5114/ceji.2021.111753>.
 31. Shen, W., Song, Z., Zhong, X., Huang, M., Shen, D., Gao, P., Qian, X., Wang, M., He, X., Wang, T., Li, S., & Song, X. (2022, 07/08). Sangerbox: A comprehensive, interaction-friendly clinical bioinformatics analysis platform [Commentary]. *iMeta*, 1(3), e36. <https://doi.org/10.1002/imt2.36>.
 32. Bonnans, C., Chou, J., & Werb, Z. (2014). Remodelling the extracellular matrix in development and disease. *Nature Reviews Molecular Cell Biology*, 15(12), 786–801. <https://doi.org/10.1038/nrm3904>.

33. Turajlic, S., & Swanton, C. (2016). Metastasis as an evolutionary process. *Science (New York N Y)*, 352(6282), 169–175. <https://doi.org/10.1126/science.aaf2784>.
34. Anderson, N., & Simon, M. (2020). The tumor microenvironment. *Current Biology: CB*, 30(16), R921–R925. <https://doi.org/10.1016/j.cub.2020.06.081>.
35. Maishi, N., & Hida, K. (2017, Oct). Tumor endothelial cells accelerate tumor metastasis. *Cancer Science*, 108(10), 1921–1926. <https://doi.org/10.1111/cas.13336>.
36. Wieland, E., Rodriguez-Vita, J., Liebler, S. S., Mogler, C., Moll, I., Herberich, S. E., Espinet, E., Herpel, E., Menuchin, A., Chang-Claude, J., Hoffmeister, M., Gebhardt, C., Brenner, H., Trumpp, A., Siebel, C. W., Hecker, M., Utikal, J., Sprinzak, D., & Fischer, A. (2017). Endothelial Notch1 activity facilitates metastasis. *Cancer Cell*, 31(3), 355–367. <https://doi.org/10.1016/j.ccell.2017.01.007>.
37. Chen, Y., McAndrews, K., & Kalluri, R. (2021). Clinical and therapeutic relevance of cancer-associated fibroblasts. *Nature Reviews Clinical Oncology*, 18(12), 792–804. <https://doi.org/10.1038/s41571-021-00546-5>.
38. Hong, L., Du, X., Li, W., Mao, Y., Sun, L., & Li, X. (2018, Sep). EndMT: A promising and controversial field. *European Journal of Cell Biology*, 97(7), 493–500. <https://doi.org/10.1016/j.ejcb.2018.07.005>.
39. Ridge, S., Sullivan, F., & Glynn, S. (2017). Mesenchymal stem cells: Key players in cancer progression. *Molecular cancer*, 16(1), 31. <https://doi.org/10.1186/s12943-017-0597-8>.
40. Tavora, B., Mederer, T., Wessel, K. J., Ruffing, S., Sadjadi, M., Missmahl, M., Ostendorf, B. N., Liu, X., Kim, J. Y., Olsen, O., Welm, A. L., Goodarzi, H., & Tavazoie, S. F. (2020, Oct). Tumoural activation of TLR3-SLIT2 axis in endothelium drives metastasis. *Nature*, 586(7828), 299–304. <https://doi.org/10.1038/s41586-020-2774-y>.
41. Liu, J., Hou, W., Guan, T., Tang, L., Zhu, X., Li, Y., Hou, S., Zhang, J., Chen, H., & Huang, Y. (2018, May). Slit2/Robo1 signaling is involved in angiogenesis of glomerular endothelial cells exposed to a diabetic-like environment. *Angiogenesis*, 21(2), 237–249. <https://doi.org/10.1007/s10456-017-9592-3>.
42. Chen, Q., Zhou, X., Hou, R., Zhou, Z., Wang, Z., Chen, Y., Weng, J., & Xu, J. (2021, Sep). Aminophylline modulates the permeability of endothelial cells via the Slit2-Robo4 pathway in lipopolysaccharide-induced inflammation. *Exp Ther Med*, 22(3), 1042. <https://doi.org/10.3892/etm.2021.10474>.
43. Gohrig, A., Detjen, K. M., Hilfenhaus, G., Korner, J. L., Welzel, M., Arsenic, R., Schmuck, R., Bahra, M., Wu, J. Y., Wiedenmann, B., & Fischer, C. (2014, Mar 1). Axon guidance factor SLIT2 inhibits neural invasion and metastasis in pancreatic cancer. *Cancer Res*, 74(5), 1529–1540. <https://doi.org/10.1158/0008-5472.CAN-13-1012>.
44. Zegeye, M., Lindkvist, M., Fälker, K., Kumawat, A., Paramel, G., Grenegård, M., Sirsjö, A., & Ljungberg, L. (2018). Activation of the JAK/STAT3 and PI3K/AKT pathways are crucial for IL-6 trans-signaling-mediated pro-inflammatory response in human vascular endothelial cells. *Cell Communication and Signaling: CCS*, 16(1), 55. <https://doi.org/10.1186/s12964-018-0268-4>.

Publisher's Note Springer Nature remains neutral with regard to jurisdictional claims in published maps and institutional affiliations.

Springer Nature or its licensor (e.g. a society or other partner) holds exclusive rights to this article under a publishing agreement with the author(s) or other rightsholder(s); author self-archiving of the accepted manuscript version of this article is solely governed by the terms of such publishing agreement and applicable law.